unclassified

MENTATION PAGE

Form Approved OMB No. 0704-0188

1a. RESTRICTIVE MARKINGS

2a. SECURITY CLASSIFICATION AUTHORITY

3. DISTRIBUTION/AVAILABILITY OF REPORT
This document has been approved for public release and sale; its distribution is unlimited.

2b. DECLASSIFICATION/DOWNGRADING SCHEDULE

4. PERFORMING ORGANIZATION REPORT NUMBER(S)

5. MONITORING ORGANIZATION REPORT NUMBER(S)

6a. NAME OF PERFORMING ORGANIZATION: General Motors

6b. OFFICE SYMBOL (If applicable):

7a. NAME OF MONITORING ORGANIZATION: Office of Naval Research (Dr. Dan Harris)

6c. ADDRESS (City, State, and ZIP Code): R&D Center, 1-6, Physical Chemistry Dept, Warren, MI 48090-9055

7b. ADDRESS (City, State, and ZIP Code): Code 3854, Naval Air Warfare Center, China Lake, CA 93355

8a. NAME OF FUNDING/SPONSORING ORGANIZATION: Office of Naval Research

8b. OFFICE SYMBOL (If applicable):

9. PROCUREMENT INSTRUMENT IDENTIFICATION NUMBER

8c. ADDRESS (City, State, and ZIP Code): 800 N. Quincy St., Arlington, VA 22217-5000

10. SOURCE OF FUNDING NUMBERS

PROGRAM ELEMENT NO.	PROJECT NO.	TASK NO.	WORK UNIT ACCESSION NO.

11. TITLE (Include Security Classification): Effects of Pressure on Diamond Formation

12. PERSONAL AUTHOR(S): Stephen J Harris and Anita M. Weiner

13a. TYPE OF REPORT	13b. TIME COVERED	14. DATE OF REPORT (Year, Month, Day)	15. PAGE COUNT
Technical	FROM ____ TO ____	93/9/27	34

16. SUPPLEMENTARY NOTATION

17. COSATI CODES			18. SUBJECT TERMS (Continue on reverse if necessary and identify by block number)
FIELD	GROUP	SUB-GROUP	

19. ABSTRACT (Continue on reverse if necessary and identify by block number)

The first measurements of the effects of pressure on the kinetics and quality of diamond films grown with hot filament chemical vapor deposition are reported. Pressure affects growth kinetics largely because it affects heat transfer between the filament and the substrate and because it affects transport of precursors to the growing surface. H and CH_3 concentrations at the growth surfaces are determined with our recombination enthalpy technique combined with appropriate transport analyses. The growth rate rises and then falls with increasing pressure, although there is a saturation in the concentration of CH_3 and atomic H at the surface. The fall in growth rate at higher pressure is explained with our chemical kinetics model as due to an increase in substrate temperature at higher pressures. Since the rate of thermal desorption of the CH_3 precursor increases more rapidly with temperature than the competing rate of its incorporation, and since these two rates are comparable, higher substrate temperatures lower incorporation rates, and the growth rate decreases.

20. DISTRIBUTION/AVAILABILITY OF ABSTRACT
☒ UNCLASSIFIED/UNLIMITED ☐ SAME AS RPT. ☐ DTIC USERS

21. ABSTRACT SECURITY CLASSIFICATION: unclassified

22a. NAME OF RESPONSIBLE INDIVIDUAL: Stephen J Harris

22b. TELEPHONE (Include Area Code): 313-986-1305

22c. OFFICE SYMBOL

DD Form 1 s are obsolete. SECURITY CLASSIFICATION OF THIS PAGE

Pressure and Temperature Effects on the Kinetics and Quality of Diamond Films

by

Stephen J. Harris

and

Anita M. Weiner

Physical Chemistry Dept., General Motors R& D Center

30500 Mound Road, PO Box 9055, Warren, MI 48090-9055

Submitted to *Journal of Applied Physics*

ABSTRACT

The first measurements of the effects of pressure on the kinetics and quality of diamond films grown with hot filament chemical vapor deposition are reported. Pressure affects growth kinetics largely because it affects heat transfer between the filament and the substrate and because it affects transport of precursors to the growing surface. H and CH_3 concentrations at the growth surfaces are determined with our recombination enthalpy technique combined with appropriate transport analyses. The growth rate rises and then falls with increasing pressure, although there is a saturation in the concentration of CH_3 and atomic H at the surface. The fall in growth rate at higher pressure is explained with our chemical kinetics model as due to an increase in substrate temperature at higher pressures. Since the rate of thermal desorption of the CH_3 precursor increases more rapidly with temperature than the competing rate of its incorporation, and since these two rates are comparable, higher substrate temperatures lower incorporation rates, and the growth rate decreases. Previously measured Arrhenius plots for diamond growth kinetics are explained quantitatively. The quality of the diamond, as determined using Raman and SEM data, falls with increasing pressure and substrate temperature. For the first time, this decline in quality is correlated with experimental temperature, H:CH_3 ratio, and C_2H_2 concentration measurements.

INTRODUCTION

A considerable amount of information has been accumulated recently in hot filament chemical vapor deposition (HFCVD) diamond systems[1,2,3,4,5]. But surprisingly, there are hardly any data for HFCVD systems at pressures other than about 20 torr[6,7,8]. While it may be that pressures much lower than 20 torr are avoided because the growth rates are low, it is less obvious why much higher pressures should be avoided in HFCVD systems. For example, one model for diamond growth[9] predicts sharply higher growth rates at 50 torr than at 20 torr. In this work we analyze diamond formation as a function of pressure between 5 and 60 torr. The results are interpreted in terms of some of the models that have been proposed[2,10,11,12] to understand diamond CVD.

EXPERIMENTAL

The growth system was a vertical 3.8 cm diameter quartz tube through which flowed a mixture of 0.75% CH_4 in H_2. The pressure ranged from 5 to 60 torr and was controlled mainly by adjusting the flow controllers. Cold gas velocities were in the range 4 to 20 cm/s, implying diffusion-controlled transport (Peclet numbers substantially less than 1) near the substrate for all cases. The coiled 250 μm diameter tungsten filament was maintained at a color temperature of 2400 ± 25 K, which required a small increase in filament current as the pressure increased. The substrate for the growth rate measurements was a 200 μm diameter platinum wire suspended 5 to 6 mm above the filament on a microbalance[7,8]. The microbalance

measurements were made after some hours of growth, by which time the diameter for the diamond-coated wire was between 250 and 350 μm, as measured with an SEM. In order to account for the changing substrate surface area, each measurement at a given pressure was preceded or followed (usually both) by a measurement at 20 torr. We report growth rates relative to 20 torr. The substrate temperature was determined as a function of pressure in separate experiments using a surrogate 250 μm diameter diamond-coated Pt/90% Pt-10% Rh thermocouple placed at the same location. H atom concentrations were determined from the recombination enthalpy technique that we developed[13] by measuring the temperature of a 50 μm diameter Pt/90%Pt-10%Rh probe thermocouple coated with a thin diamond layer. Mass spectral measurements for CH_4 and C_2H_2 were made using a quartz microprobe, as described previously[8,14].

For estimating gas phase temperatures we use the results of Meier et al.[15,16], who took laser induced fluorescence (LIF) measurements at 4, 10, 20, and 30 torr near a straight 400 μm diameter filament. In order to evaluate the effects of different filament geometry in our experiment (coiled 250 μm filament), we made thermocouple measurements in 99% He/1% CH_4 mixtures between 5 and 60 torr with both sizes and shape filaments. By using He rather than H_2 we avoided the effects of radical recombination on the thermocouple.

RESULTS

Figure 1 shows that the growth rate goes through a maximum near 30 torr,

falling by about 40% between 30 and 60 torr. Zhu et al.[6] also observed a rise and then a fall in growth rate with pressure in their plasma assisted CVD system, but in their system it was not clear whether it was the gas or surface chemistry or the plasma physics which was being affected by pressure. Figures 2 and 3 show Raman spectra and SEM micrographs of films grown at 10, 23, and 44 torr. The background luminescence and sp^2 signal at 1550 cm^{-1} are non-negligible in Figure 2 at the higher pressures, although the diamond line at 1333 cm^{-1} is always strongly dominant. The line widths are 4.95, 10.8, and 14.1 cm^{-1}, respectively. (Instrumental line width $\sim$ 3 cm^{-1}). The diamond surfaces become rougher on a micron scale at higher pressures.

The only previous measurements of the gas phase temperature in a HFCVD environment were made by Meier et al[15,16]. This group used LIF to measure the gas temperature as a function of pressure and distance from a straight 400 μm diameter filament. Our measurements in He/CH_4 mixtures show only a small effect ($<$ 50 K) on the gas temperature from changing filament size and geometry, so we have used their data to estimate our gas temperatures. The LIF data show a relatively rapid rate of increase in temperature between 4 and 20 torr, and a smaller rate of increase between 20 and 30 torr (see symbols in Figure 4). Because there are no experimental gas temperature data for pressures above 30 torr, and since the He measurements and the substrate temperature measurements (Figure 5) show a similar flattening out of temperature with pressure above 30 torr, we have extrapolated the gas temperature data to 60 torr, using the He temperature measurements as a guide, as shown in Figure 4. Fortunately, the analysis is hardly

affected by uncertainty in the gas phase temperature (see below).

The concentrations of CH_4 and C_2H_2 are shown as functions of pressure in Figure 6. The CH_4 concentration is strongly affected by thermal diffusion[1,14] near the filament, which accounts in part for its low value relative to the input concentration. The C_2H_2 concentration is approximately independent of distance from the filament[14].

ANALYSIS

Our models have been successful in predicting experimentally observed growth rates in a variety of systems[2,10] including HFCVD, low- and atmospheric-pressure flames, dc, rf and thermal[17] plasmas. Previously, this model was applied only to systems with a substrate temperatures close to $T_{sub} = 1200$ K, but Figure 5 shows that in these experiments the surface temperature varied by more than 250 K. The ability of the model to account for variations in T_{sub} has not previously been tested.

H Atom Concentration Measurements

In order to obtain $[H]_{sub}$ (concentration of H at the substrate surface, required by the model) we first use the 50 μm probe thermocouple to find $[H]_{tc}$, the concentration at the probe thermocouple surface. From a transport analysis we then determine $[H]_{bulk}$, the concentration in the bulk gas, far from any perturbation by a substrate. (We note that using a wire of 150 micron diameter gave the same values for bulk [H].) Finally, we derive the concentration at the growth substrate using a second transport analysis.

According to our analysis for the recombination enthalpy technique, the concentration of atomic hydrogen at the surface of a "sufficiently fine" wire (which can be a thermocouple) is given by[13]

$$[H]_{tc} = \left(\frac{8\epsilon\sigma}{\gamma_H v \Delta E} \right) T_{tc}^4, \tag{1}$$

where $\gamma_H = 2.0\, e^{-6020/RT}$ is the probability for H destruction on the (diamond-coated) thermocouple surface[18]; ΔE is the heat of recombination forming H_2 from 2 H atoms; v is the velocity of an H atom; σ is the Stefan-Boltzmann constant; T_{tc} is the thermocouple temperature; and ϵ is the emissivity of the diamond-coated wire. We found previously[13] that a roughly 100 μm thick diamond film increased the emissivity of a platinum wire by about 20%. Since the film on the probe thermocouple wire was only a few microns thick, we set $\epsilon = \epsilon(Pt)$. "Sufficiently fine" means small enough so that heat transfer from the gas, radiation heating from the filament, and conduction along the wire are small compared to heat liberated by H recombination and heat lost by radiation. Heat transfer becomes very inefficient as the mean free path of the gas molecules approaches the substrate size. Our experience shows that at 20 torr (H mean free path $\sim$ 70 μm) a thermocouple with a diameter of 130 μm is satisfactory. Since the present experiments involved pressures as high as 60 torr, we used a thermocouple with a 50 μm diameter, which was the thinnest practical size.

H atom destruction at the thermocouple surface is partly transport limited, which means that $[H]_{tc}$ is lower than $[H]_{bulk}$. $[H]_{tc}$ and $[H]_{bulk}$ can be related by treating the wire as a long cylinder in a cylindrically symmetrical field of H atoms

and by setting the diffusion rate of H atoms to the wire equal to their destruction rate at the wire surface. The result is[13]

$$\frac{[H]_{tc}}{[H]_{bulk}} = 1 + \left[\frac{\ln(R_t/R_{tf})}{\ln(R_{tf}/R_t) + (4D_H/\gamma_H v R_t)}\right] \qquad (2)$$

where R_{tf} is a reference distance such as the distance between the thermocouple and the filament, R_t is the radius of the diamond-coated wire, and D_H is the diffusion coefficient of an H atom. $[H]_{tc}/[H]_{bulk}$ drops from about 0.9 to 0.5 as the pressure increases from 5 to 60 torr. Open symbols in Figure 7 show that $[H]_{bulk}$ rises slowly with pressure. The only previous absolute measurements of $[H]_{bulk}$ were made by Meier et al.[19] using LIF. They found $[H]_{bulk}$ to be independent of pressure between 10 and 60 torr. The discrepancy with the present results may be due in part to experimental differences between their system and ours. For example, Meier et al. used a 2 mm diameter filament for these measurements, eight times thicker than our filament. In their analysis they took the gas temperature at 10 torr to be about 1800 K, more than 1000 K higher than our temperature. However, the most important difference is probably our use of a single-filament optical pyrometer, which measures only the color temperature rather than the true temperature of the filament. We found that at constant filament current, the color temperature of our filament decreased by nearly 100 K between 5 and 60 torr, possibly reflecting changes in heat transfer (a real change in filament temperature) or in the emissivity[20] (an artifact of our measurement technique). At constant filament current our measured $[H]_{bulk}$ was independent of pressure. Thus, relatively small uncontrolled variations in the temperature of our filament probably are responsible for the discrepancy.

We note that Meier et al. did make some measurements with a thinner (300 μm diameter) filament. For that case, their measured H atom concentration is the same as ours to within experimental error.

From $[H]_{bulk}$, we next calculate $[H]_{sub}$, the concentration at the substrate surface during growth. Since the wire used in the microbalance experiments is thicker than the (50 μm) probe thermocouple, it perturbs the local H concentration to a greater extent. Using Eqn (2) with $R_t = 150$ μm, we find that $[H]_{sub}/[H]_{bulk}$ varies from 0.7 to 0.2 as the pressure increases from 5 to 60 torr. $[H]_{sub}$ is plotted as a function of pressure with solid symbols in Figure 7.

CH_3 Radical Concentration Measurements

In order to determine $[CH_3]_{bulk}$ we take advantage of the fact that CH_3 and CH_4 are strongly coupled through the fast reaction

$$CH_3 + H_2 = CH_4 + H, \qquad (I)$$

which is in partial equilibrium except near the substrate[21]. Therefore, $[CH_3]_{bulk} = K_{eq}[CH_4][H]_{bulk}/[H_2]$. Because of the large uncertainty in T_{gas} for pressures above 30 torr, we are fortunate that K_{eq} changes only slightly with T_{gas}, by about 5% for a 100 K temperature change. $[CH_3]_{bulk}$ is shown with open symbols in Figure 7. Our value at 20 torr, 2.8×10^{-11} moles/cm^3, is very close to the value measured recently at 20 torr by Menningin et al.[22] using UV absorption. The analysis used in the present work for [CH_3] is based on (i) the recombination enthalpy technique to determine $[H]_{tc}$; (ii) Eqn (2) to derive $[H]_{bulk}$; and (iii) partial equilibrium of I to derive $[CH_3]_{bulk}$. Thus, the excellent agreement between our results and the direct

measurements of Menningin et al.[22] lends support to these three components of our analysis. (Mennin- n et al.[22] measured a strong dependence of $[CH_3]$ on the filament temperature which is similar to that observed[13] for [H] a s a function of filament temperature. The reason for the similarity is the rapid equilibration in the gas phase of I, which forces $[H]_{bulk}$ and $[CH_3]_{bulk}$ to follow one another.)

The relationship between $[CH_3]_{bulk}$ and $[CH_3]_{sub}$ is somewhat more complex than that between $[H]_{bulk}$ and $[H]_{sub}$ since $[CH_3]_{sub}$ is affected not only by destruction at the surface but also by gas phase reactions—mainly I—fast enough to deplete CH_3 as it diffuses through the H concentration gradient, but not fast enough to maintain partial equilibrium of I all the way in to the substrate surface[23]. Therefore, we solve the species balance equation,

$$D_{CH_3}\left[\frac{\partial^2[CH_3]}{\partial r^2}+\left(\frac{1}{r}\right)\frac{\partial[CH_3]}{\partial r}\right]=k_I[CH_3][H_2]-k_{-I}[CH_4][H], \qquad (3)$$

using the PARA code of Verbrugge and Gu[24]. In this equation, D_{CH_3} is the diffusion coefficient, r is the distance from the substrate, and k_I and k_{-I} are the forward and reverse rate constants for I. Destruction of CH_3 by reaction with the diamond substrate, which makes a small but non-negligible contribution, is treated as a boundary condition using the approximate destruction probability measured by Krasnoperov et al.[18], $\gamma_{CH_3}=1.3\,e^{-10640/RT}$. The results are shown with solid symbols in Figure 7.

DISCUSSION

Growth Rate Modeling

In order to interpret the experimental results shown in Figure 1 we have used a model that we proposed for growth on the (100)-(2×1):H dimer reconstructed face of diamond[2]. This surface has been observed experimentally[25,26] and examined with molecular mechanics[27]. The model includes a pair of previously proposed mechanisms[10,28] which operate sequentially: half of the growth is accounted for by insertion into dimer bonds, while the other half is accounted for by addition across troughs between dimer bonds. (Because the dimer mechanism is so much faster than the trough mechanism, the trough mechanism alone gives nearly the same predictions as the combined mechanism.) The dashed line in Fig 1 shows the predictions of the model, also scaled to 1.0 at 20 torr. Agreement is rather good, considering the lack of adjustable parameters in the model, with both experiment and the model showing a maximum followed by a gradual decrease in growth rate with pressure.

According to the model, the rise in the growth rate at low pressures is due mainly to the increase in $[CH_3]_{sub}$ as well as the increase in T_{sub}. The decline in the growth rate at higher pressures, where both $[H]_{sub}$ and $[CH_3]_{sub}$ saturate, is due to a higher substrate temperature. (T_{sub} is near 1200 K at 30 torr.) The rather complex effect that substrate temperature has is explained as follows. The model postulates that once a CH_3 radical adds to the diamond surface, it has a choice: it can either desorb thermally or it can undergo further reactions with gas phase H

atoms that lead to incorporation of its carbon into the lattice. Since the desorption and incorporation rates can be on the same order of magnitude, the growth rate depends sensitively on the branching ratio into these two pathways. The branching ratio is strongly temperature dependent because thermal desorption (breaking a C-C bond) has a very much higher activation energy—say, 85 kcal/mole—than the incorporation reactions (H abstraction)—say, 5-10 kcal/mole. Thus, at low substrate temperatures (corresponding to low pressures in this work, see Figure 5) desorption of CH_3 is relatively slow, and most of the CH_3 precursor which adsorbs is eventually incorporated into the diamond. However, at higher substrate temperatures thermally activated desorption becomes increasingly important, reducing the growth rate. The model shows that increased desorption relative to incorporation rates in this temperature range explains the decrease in growth rates at high pressures.

Thermal desorption also explains the decrease in the growth rate observed previously—but not explained—in HFCVD systems above 1200 K[29], since the growth rate decreases if the desorption lifetime of CH_3 is shorter than the time required for incorporation. Finally, since the CH_3 addition and incorporation rates increase with $[H]$ and $[CH_3]$ while the desorption rate is independent of the gas phase composition, our analysis predicts that the temperature at which the growth rate peaks should be higher for systems with high concentrations of H and CH_3. For example, in atmospheric pressure oxyacetylene flames $[H]_{sub}$ and $[CH_3]_{sub}$ are about 10^{-8} and 10^{-9} moles/cm^3, respectively[21], much higher than the concentrations in HFCVD systems. Thus, the model accounts for the observation that

growth rates remain high in these flames at very high temperatures[30].

Pressure also plays other, more direct roles in determining growth rates. Most importantly, it controls the concentration gradients for H and CH_3, first discussed by Goodwin[21], because the diffusion coefficients are pressure dependent. Pressure affects the radical site fraction on the surface, f^*, through a more subtle interaction. f^* is determined[10] by a competition between H abstraction

$$C-H + H^{gas} = C^* + H_2^{gas} \qquad (II)$$

and addition,

$$C^* + H^{gas} = C-H, \qquad (III)$$

where $C-H$ represents a hydrogen-terminated carbon site on the diamond surface, and C^* represents a radical site. For pressures below 20 torr and T_{sub} below 1200 K, II and III are nearly irreversible, and at steady state

$$f^* = \frac{k_{II}}{k_{II} + k_{III}}. \qquad (IV)$$

However, the reverse of II becomes increasingly important as the temperature increases and as $[H_2]$ increases relative to [H], both of which happen at higher pressure. Thus, at high enough pressures f^* decreases compared to the prediction of IV. With fewer sites available for CH_3 addition, the growth rate is lowered.

The shape of the data in Figure 1 reflects the competing effects of adsorption, desorption, and incorporation reactions as the pressure and substrate temperature change. The model (dashed curve) predicts a maximum in the growth rate between 15 and 20 torr (T_{sub} = 1100 K) compared to approximately 30 torr (T_{sub} = 1200 K)

observed in the experiment. One possible source for this discrepancy could be an underestimate for the bond strength between CH_3 and the lattice. The model would predict a peak in the growth rate at 1200 K—30 torr—if the bond strength assumed in the model were increased by roughly 10 kcal/mole or if there were a 10 kcal/mole barrier in the entrance channel for addition of methyl to the surface. (Our present model assumes no barrier.) The maximum in the Arrhenius plot of Kondoh[29] is also reproduced quantitatively by the model if a greater bond strength is used. However, it is important to point out that the morphology of the surface also varies with pressure, at least on a micron scale, as seen in Figure 3. This variation in morphology—not accounted for in the model—could also be a source for the discrepancy. Finally, we should point out that although in this work the growth rate maximizes between 20 and 30 torr, with other experimental parameters (filament power, filament-substrate distance, substrate dimensions, etc.) the growth rate would in general maximize at other pressures.

Recently, Goodwin[11], Butler and Wooden[12], and Kim and Cappelli[31] have constructed reduced or generic growth mechanisms which describe some of the features of our detailed mechanism and which can lead to simplified or closed form solutions for the growth rate in terms of $[CH_3]$ and [H]. A typical approximation in these reduced mechanisms is the assumption that ΔG for all reactions of a particular class (abstraction, addition, etc.) is the same. For Goodwin's reduced mechanism, which reproduces the detailed mechanism (and experimental data) very well at 1200 K, another simplifying assumption is that the reactions which lead to incorporation of a CH_3 carbon can be represented with a single global

step whose rate is proportional to [H] and to a rate constant k_i. In contrast, more detailed mechanisms[2,32] generally require the presence of radical site pairs, for which the effective activation energy of formation is twice that for forming single radical sites. Although it is not yet clear whether reduced mechanisms can reproduce experimental data over a wide temperature range, it is interesting that if Goodwin's k_i is given an activation energy of 6-10 kcal/mole, corresponding to a typical abstraction reaction, the reduced mechanism predicts a monotonic fall in growth rate with pressure in our system. However, if k_i is given an activation energy of 12-20 kcal/mole, twice that for forming single radical sites, the full model—and the present experimental results—can be fit well.

Corat and Goodwin[33] have recently found that the dependence of $[CH_3]$ on the substrate temperature can be described with an activation energy of approximately 4 kcal/mole. Since the growth rate is first order in $[CH_3]$[7], the effective activation energy for growth would be the sum of the activation energy for $[CH_3]$ (4 kcal/mole) and the activation energy for production of radical site pairs(12-20 kcal/mole), or roughly 20 kcal/mole. This result is in excellent agreement with the experimental results of Kondoh at low temperatures (< 1200 K), where the effects of thermal desorption are small. Thus, both the low and high temperature parts of Kondoh's Arrhenius plot are accounted quantitatively for with our model.

Effects of Pressure on Diamond Quality

Although a precise definition of "quality" is not available, high quality is often associated with smooth surfaces and also with certain features in the Raman spectra, such as a narrow 1333 cm^{-1} diamond line and low intensities for both the

background and the sp^2 peak at 1550 cm^{-1}. It has been widely observed that quality declines as the hydrocarbon fraction in the feed gas increases, and there have been several explanations offered. Frenklach and Wang[9] proposed that aromatics such as benzene formed in the gas phase condense on the growing surface, poisoning diamond growth and promoting formation of an sp^2 component. Since aromatic concentrations increase rapidly with hydrocarbon concentration, quality would decline at higher hydrocarbon concentrations. However, it has been shown[34] that even at benzene concentrations hundreds of times higher than the $\sim$ 1 ppm observed experimentally for HFCVD systems[14], there is no measurable impact on either the growth rate or the quality of diamond films grown in a discharge flow tube downstream from the point of benzene injection. (This is true not only near the injection point but also at points far downstream, where mixing of benzene with the other gases in the flow tube was complete.) Goodwin[11] and Butler and Woodin[12] modeled quality as a competition between formation of defects and of diamond from CH_3. Both models predict that quality improves as [H] increases and $[CH_3]$ decreases. Figure 8 shows the ratio $R = [H]_{sub}/[CH_3]_{sub}$. In comparing Figs 2 and 8 we note that the higher quality at 10 torr compared to 20 torr correlates with a higher value for R. However, R changes little at still higher pressures, while quality continues to degrade. By assuming that the reaction which forms defects has a large activation energy, Butler and Woodin predict that for constant R in a HFCVD environment, quality decreases with increasing temperature for $T_{sub} > 1100$ K. Our Raman results are consistent with this prediction. Another correlation which may be of significance is the rapid increase in $[C_2H_2]$ with pres-

sure, as seen in Figure 6. Although acetylene can be a precursor for diamond[35,36], it can also be a precursor for sp^2 carbon[37].

SUMMARY

We have made the first measurements of the pressure-dependence of diamond growth kinetics in a HFCVD system. The concentrations of H and CH_3 at the substrate surface as functions of pressure were determined, and good agreement with previous, more direct, absolute concentration measurements is obtained. We used these data to model our experimental growth rate data, and again, rather good agreement with relative experimental growth rates was found. We find that the growth rate saturates and then falls above about 30 torr. The saturation in growth is due to saturation of $[H]_{sub}$ and $[CH_3]_{sub}$. A discrepancy in the pressure for peak growth could be accounted for by a stronger bond between CH_3 and the surface than was used in the model. The observed dependence of the diamond growth rates on temperature for both HFCVD and flames can be accounted for by the temperature dependence of thermal desorption of CH_3. The Raman spectra, while sparse, give the first experimental data correlating diamond quality and $[H]_{sub}/[CH_3]_{sub}$. Higher surface temperatures and C_2H_2 concentrations also correlate with lower quality in our system.

Acknowledgments

We are grateful to Dr. Thomas P[illegible] of the GM R&D Center for taking the Raman spectra and to Dr. Mark Verbrugge for use of his program to solve a

transport equation. Valuable discussions with Professor David Goodwin of Caltech are gratefully acknowledged. This work was supported in part by the Office of Naval Research.

References

[1] S. J. Harris, A. M. Weiner, and Thomas A. Perry. Measurement of stable species present during filament-assisted diamond growth. *Applied Physics Letters*, 53:1605, 1988.

[2] S. J. Harris and D. G. Goodwin. Growth on the reconstructed diamond (100) surface. *Journal of Physical Chemistry*, 97:23, 1993.

[3] D. G. Goodwin and G. G. Gavillet. Numerical modeling of the filament-assisted diamond growth environment. *Journal of Applied Physics*, 68:6393, 1990.

[4] C. J. Chu, M. P. D'Evelyn, R. H. Hauge, and J. L. Margrave. Mechanism of diamond film growth by chemical vapor deposition on diamond (100), (111), and (110) surfaces:Carbon-13 studies. *Journal of Applied Physics*, 70:1695, 1991.

[5] F. G. Celii and J. E. Butler. Diamond chemical vapor deposition. *Annual Review of Physical Chemistry*, 42:643, 1991.

[6] W. Zhu, R. Messier, and A. R. Badzian. Effects of process parameters on CVD diamond films. In J. P. Dismukes, editor, *Diamond and Diamond-like Films*, page 61, Electrochemical Society, Pennington, NJ, 1989.

[7] S. J. Harris, A. M. Weiner, and T. A. Perry. Filament-assisted diamond growth kinetics. *Journal of Applied Physics*, 70:1385, 1991.

[8] S. J. Harris and A. M. Weiner. Diamond growth rates versus acetylene con-

centrations. *Thin Solid Films*, 212:201, 1992.

[9] M. Frenklach and H. Wang. Detailed surface and gas-phase chemical kinetics of diamond deposition. *Physical Review B*, 43:1520, 1991.

[10] S. J. Harris. A mechanism for diamond growth from methyl radicals. *Applied Physics Letters*, 56:2298, 1990.

[11] D. G. Goodwin. Scaling laws for diamond chemical vapor deposition. *Journal of Applied Physics*, submitted.

[12] J. E. Butler and R. L. Woodin. Thin film diamond growth mechanisms. *Phil. Trans. R. Soc. Lond. A*, 342:209, 1993.

[13] S. J. Harris and A. M. Weiner. Reaction kinetics on diamond:Measurement of H atom destruction rates. *Journal of Applied Physics*, 74:1022, 1993.

[14] S. J. Harris, D. N. Belton, A. M. Weiner, and S. J. Schmieg. Diamond growth on platinum. *Journal of Applied Physics*, 66:5353, 1989.

[15] U. E. Meier, L. E. Hunziker, D. R. Crosley, and J. B. Jeffries. Observation of OH radicals in a filament-assisted diamond growth environment. In *Proceedings of the Electrochemistry Society*, page 202, Electrochemical Society, Pennington, NJ, May 1991.

[16] J. B. Jeffries. SRI International, Private communication.

[17] B. W. Yu, H. Hand, and S. L. Girshick. Chemical vapor deposition of diamond film with an atmospheric-pressure plasma:boundary layer chemistry. In *11'th International Symposium on Plasma Chemistry*, Loughborough, England, Au-

gust 1993.

[18] L. N. Krasnoperov, I. J. Kalinovski, D. Gutman, and H. N. Chu. Heterogeneous reaction of H atoms and CH_3 radicals on a diamond surface in the 300-1133 K temperature range. *Journal of Physical Chemistry*, submitted.

[19] U. Meier, K. Kohse-Hoinghaus, L. Schafer, and C. Klages. Two-photon excited LIF determination of H atom concentrations near a heated filament in a low pressure H_2 environment. *Applied Optics*, 29:4993, 1990.

[20] M. Sommer and F. W. Smith. Activity of tungsten and rhenium filaments in CH_4/H_2 and C_2H_2/H_2 mixtures: Importance for diamond CVD. *Journal of Materials Research*, 5:2433, 1990.

[21] D. G. Goodwin. Simulations of high-rate diamond synthesis: methyl as growth species. *Applied Physics Letters*, 59:277, 1991.

[22] K. L. Menningen, M. A. Childs, P. Chevako, H. Toyoda, L. W. Anderson, and J. E. Lawler. Methyl radical production in a hot filament CVD system. *Chemical Physics Letters*, 204:573, 1993.

[23] W. L. Hsu. Mole fractions of H, CH_3, and other species during filament-assisted diamond growth. *Applied Physics Letters*, 59:1427, 1991.

[24] M. W. Verbrugge and H. Gu. Finite difference routines for one and two dimensional problems with mesh allocation. In R. E. White, M. W. Verbrugge, and J. F. Stockel, editors, *Modeling of Batteries and Fuel Cells*, The Electrochemical Society, 1991.

[25] T. Tsuno, T. Imai, Y. Nishibayashi, K. Hamada, and N. Fujimori. Epitaxially grown diamond (001) 2x1/1x2 surface investigated by scanning tunneling microscopy in air. *Japanese Journal of Applied Physics*, 30:1063, 1991.

[26] L. F. Sutcu, C. J. Chu, M. S. Thompson, R. H. Hauge, J. L. Margrave, and M. P. D'Evelyn. Atomic force microscopy of (100), (110), and (111) homoepitaxial diamond films. *Journal of Applied Physics*, 71:5930, 1992.

[27] Y. L. Yang and M. P. D'Evelyn. Structure and energetics of clean and hydrogenated diamond (100) surfaces by molecular mechanics. *Journal of the Americal Chemical Society*, 114:2796, 1992.

[28] B. J. Garrison, E. J. Dawnkaski, D. Srivastava, and D. W. Brenner. Molecular dynamics simulations of dimer opening on a diamond 001(2x1) surface. *Scicnce*, 255:835, 1992.

[29] E. Kondoh, T. Ohta, T. Mitomo, and K. Ohtsuka. Surface reaction kinetics of diamond growth from the gas phase. *Journal of Applied Physics*, 73:3041, 1993.

[30] K. A. Snail, R. A. Weimer, and T. P. Thorpe. Flame process for the growth of large diamond crystals. In *Third International Symposium on Diamond Materials*, page to be published, Electrochemical Society, Honolulu, Hawaii, May 1993.

[31] M. H. Loh and M. A. Cappelli. Supersonic DC-Arcjet synthesis of diamond. *Diamond and Related Materials*, accepted.

[32] D. N. Belton and S. J. Harris. Growth from acetylene on a diamond (110)

surface. *Journal of Chemical Physics*, 96:2371, 1992.

[33] E. J. Corat and D. G. Goodwin. Temperature dependence of species concentrations near the substrate during diamond chemical vapor deposition. *Journal of Applied Physics*, 74, Aug 1, 1993.

[34] L. R. Martin and S. J. Harris. Do aromatic molecules inhibit diamond film growth? *Applied Physics Letters*, 59:1911, 1991.

[35] S. J. Harris and L.R. Martin. Methyl vs acetylene as diamond growth species. *Journal of Materials Research*, 5:2313, 1990.

[36] M. H. Loh and M. A. Cappelli. In A. J. Purdes, K. E. Spear, B. S. Meyerson, M. Yoder, R. Davis, and J. C. Angus, editors, *Third International Symp. Diamond Materials*, page in Press, The Electrochemical Society, Honolulu, Hawaii.

[37] S. J. Harris and A. M. Weiner. Chemical kinetics of soot particle growth. *Annual Review of Physical Chemistry*, 36:31, 1985.

Captions

1. Measured growth rate (filled circles) and predicted growth rate (dashed line) relative to that at 20 torr. Most points are averages of 2 or 3 measurements.

2. Raman spectra at 10 (bottom spectrum), 23 (middle spectrum) and 44 (upper spectrum) torr. Background luminescence and the 1333 cm^{-1} line width increase dramatically with pressure.

3. SEM of diamond films grown at 10, 23, and 44 torr.

4. Gas phase temperatures as a function of gas pressure. Solid squares are the data of Meier et al. The dashed line is the temperature dependence assumed in this work.

5. Substrate temperature as a function of gas pressure.

6. Methane and acetylene concentrations at the substrate as functions of pressure.

7. Concentrations of CH_3 and atomic H as functions of gas pressure. Open symbols are bulk concentrations, far from any perturbation by a surface. Solid symbols are concentrations at the growth substrate.

8. H:CH_3 ratio as a function of pressure.

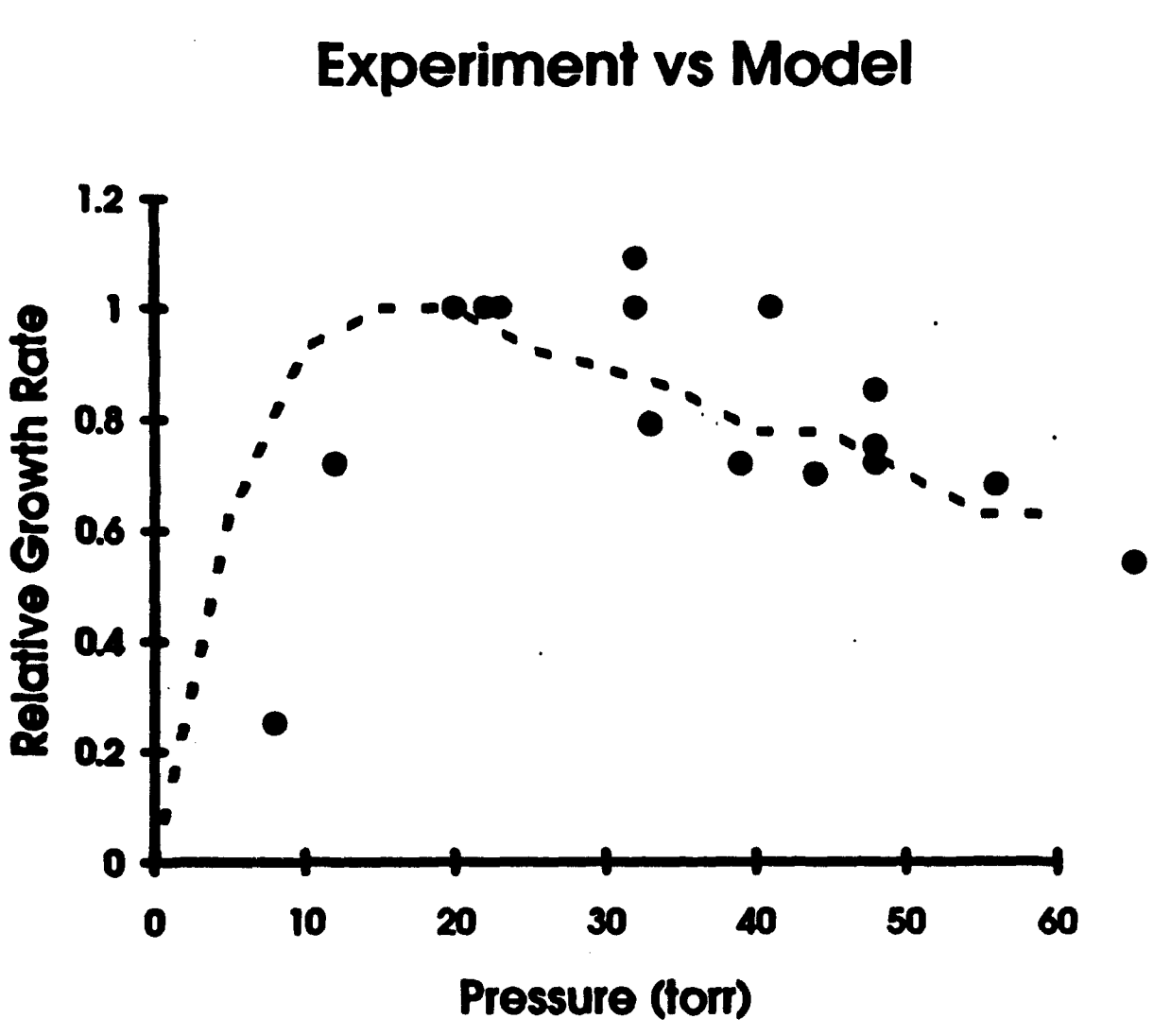
Experiment vs Model
Relative Growth Rate
1.2
1
0.8
0.6
0.4
0.2
0
0
10
20
30
40
50
60
Pressure (torr)

FIG. 1

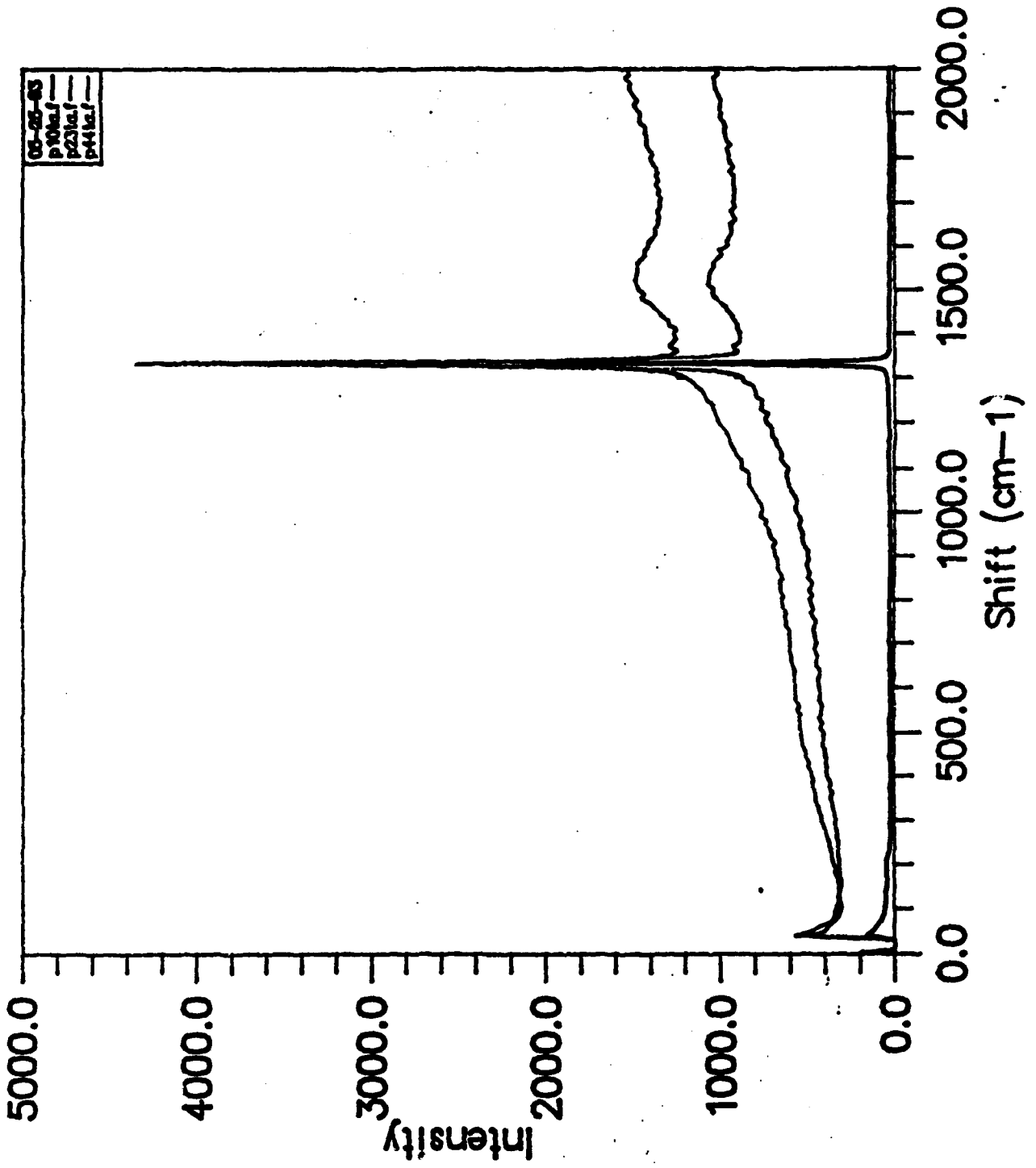

2. Raman spectra at 10 (bottom spectrum), 23 (middle spectrum) and 44 (upper spectrum) torr. Background luminescence and the 1333 cm^{-1} line width increase dramatically with pressure.

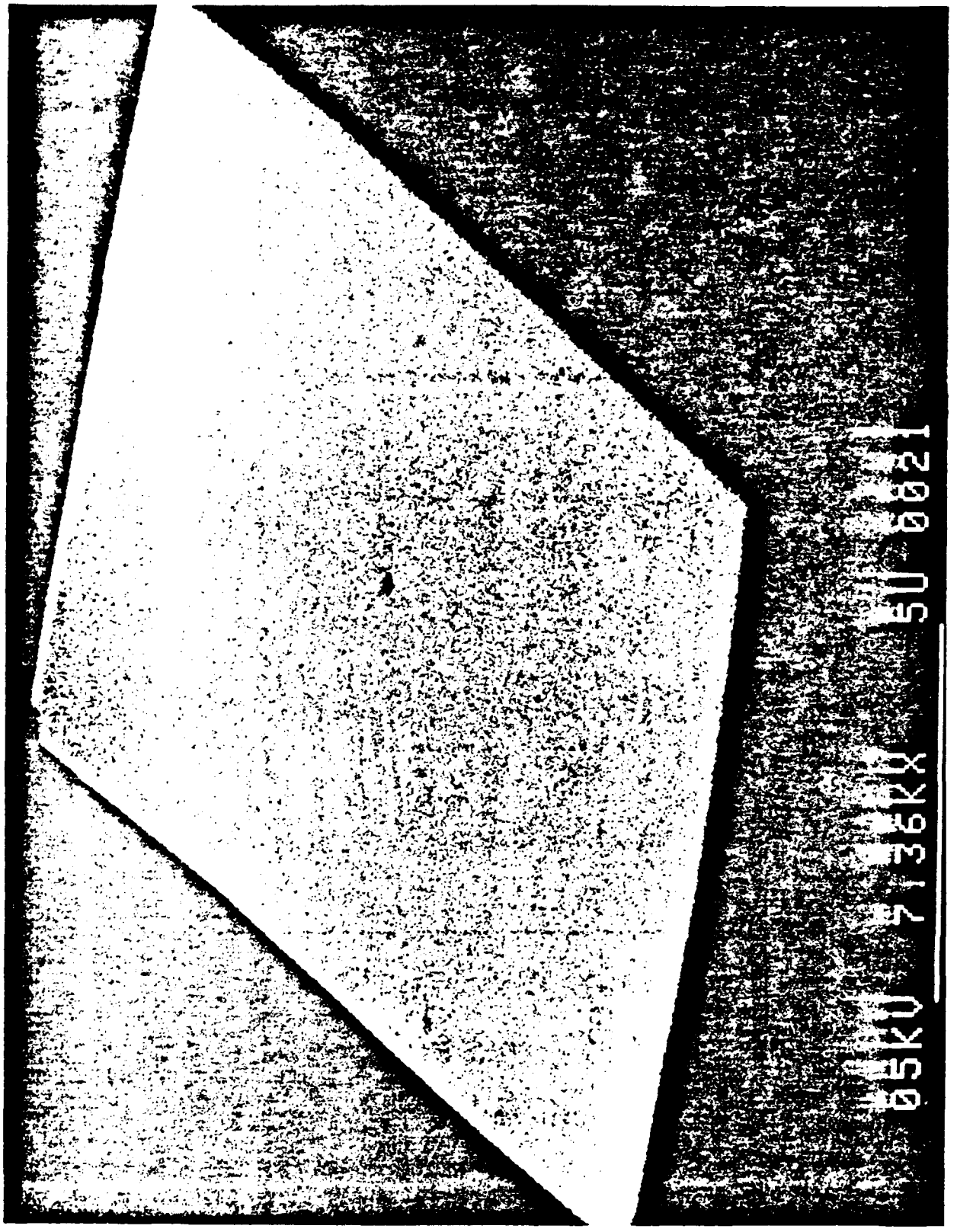

3a. SEM of diamond films grown at 10 torr.

3b. SEM of diamond films grown at 23 torr.

3c. SEM of diamond films grown at 44 torr.

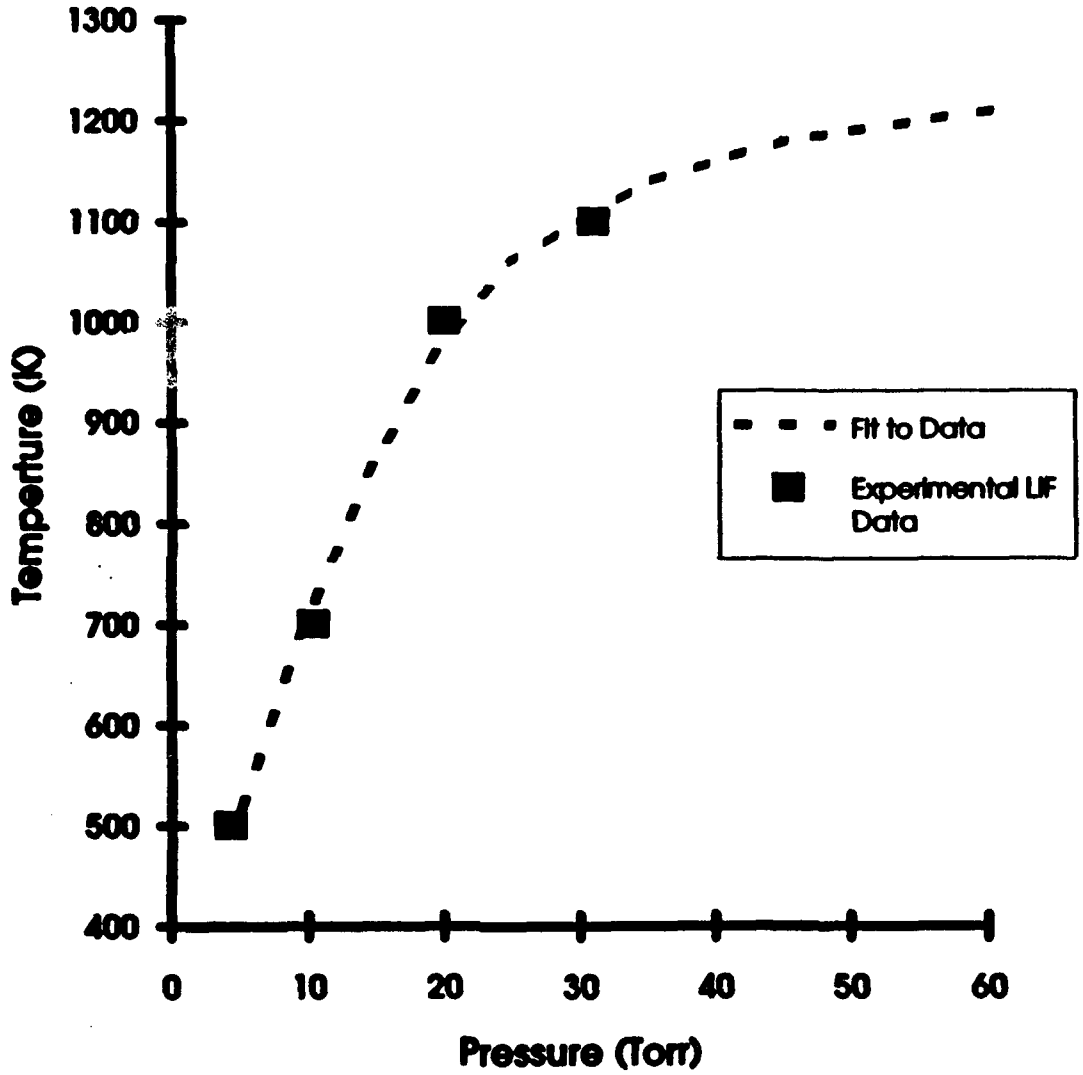
1300
1200
1100
1000
900
800
700
600
500
400
Temperture (K)
0
10
20
30
40
50
60
Pressure (Torr)
Fit to Data
Experimental LIF Data

FIG. 4

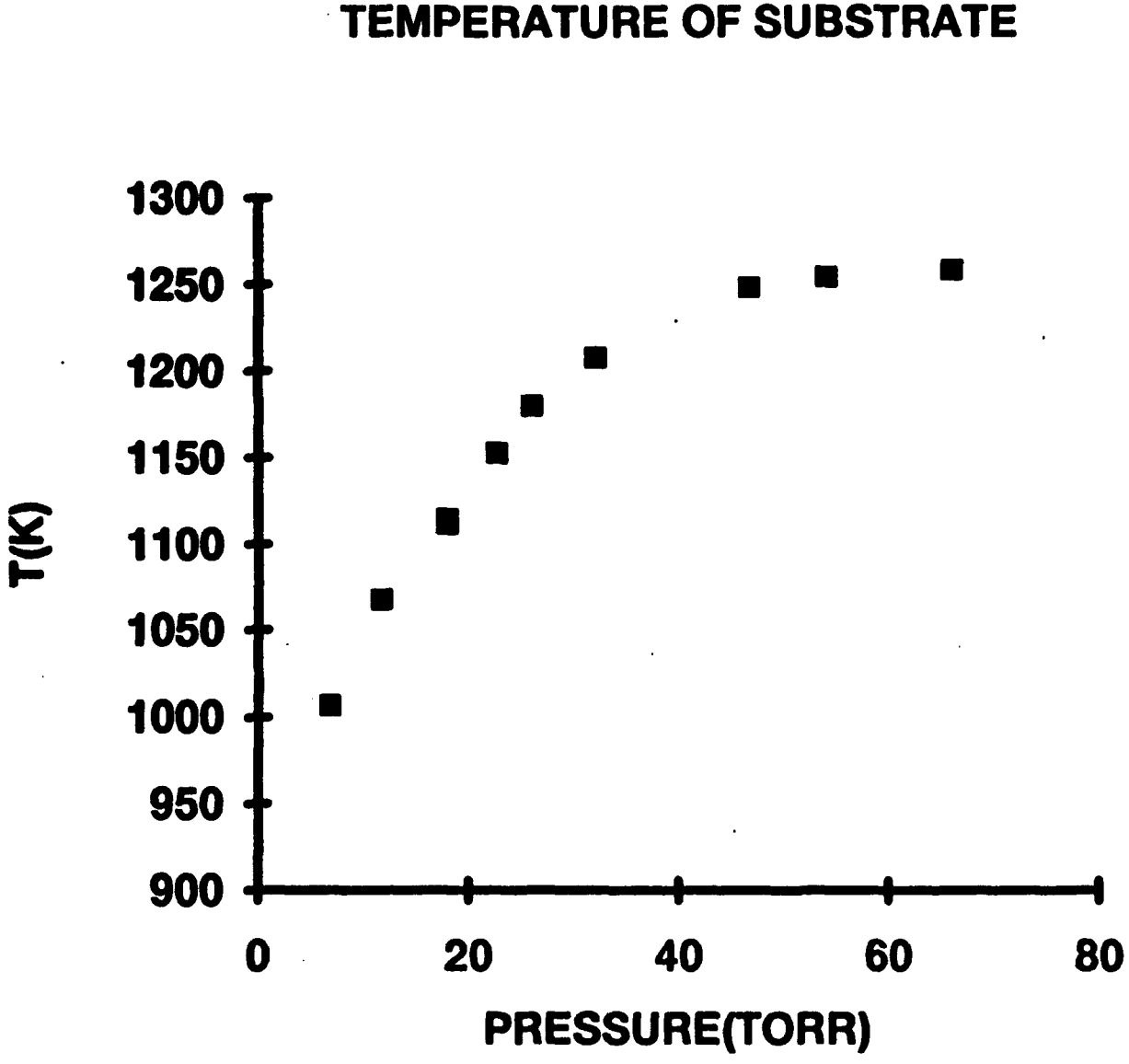
TEMPERATURE OF SUBSTRATE
1300
1250
1200
1150
1100
1050
1000
950
900
T(K)
0
20
40
60
80
PRESSURE(TORR)

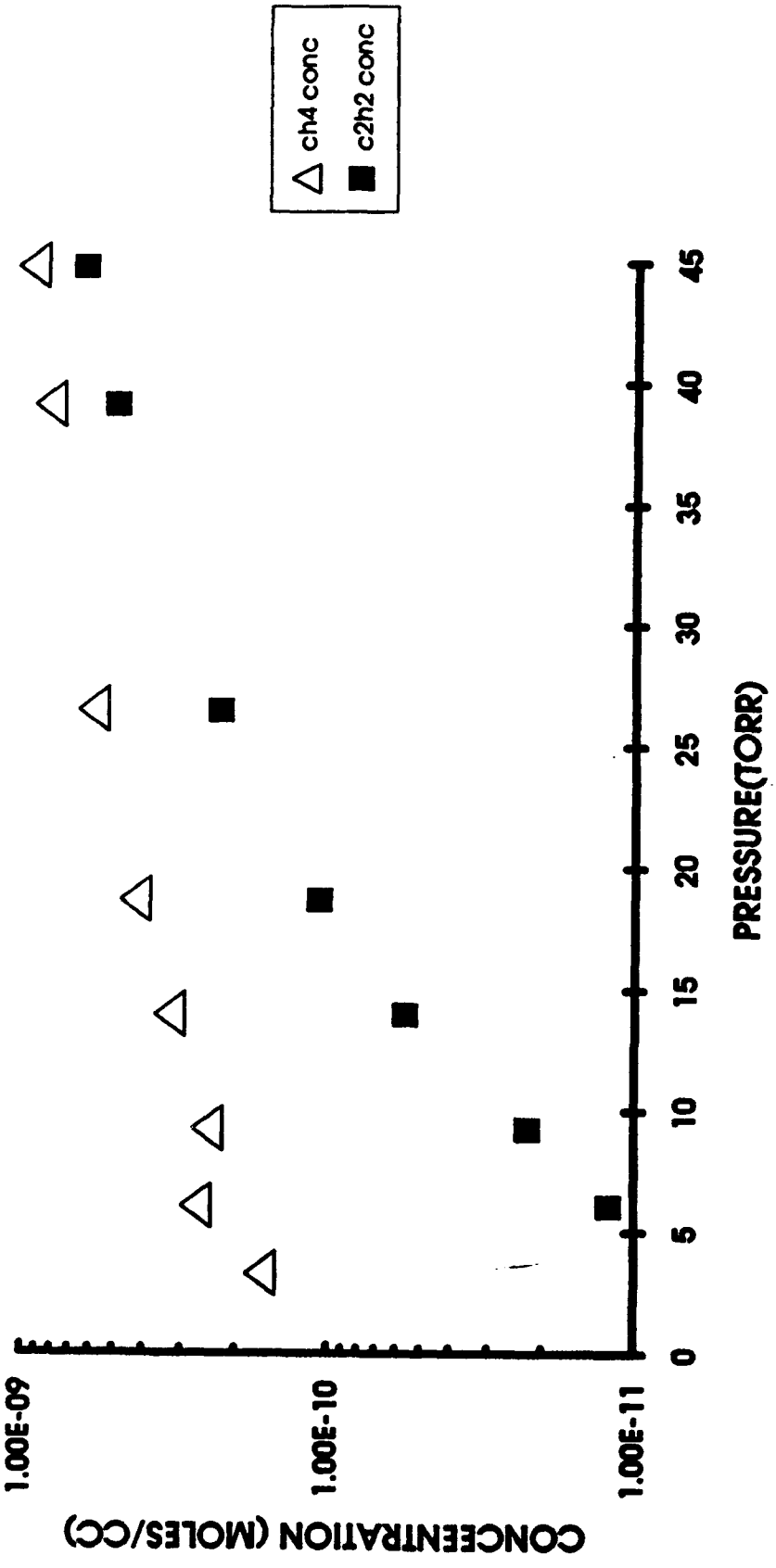

FIG. 6

6. Methane and acetylene concentrations at the substrate as functions of pressure.

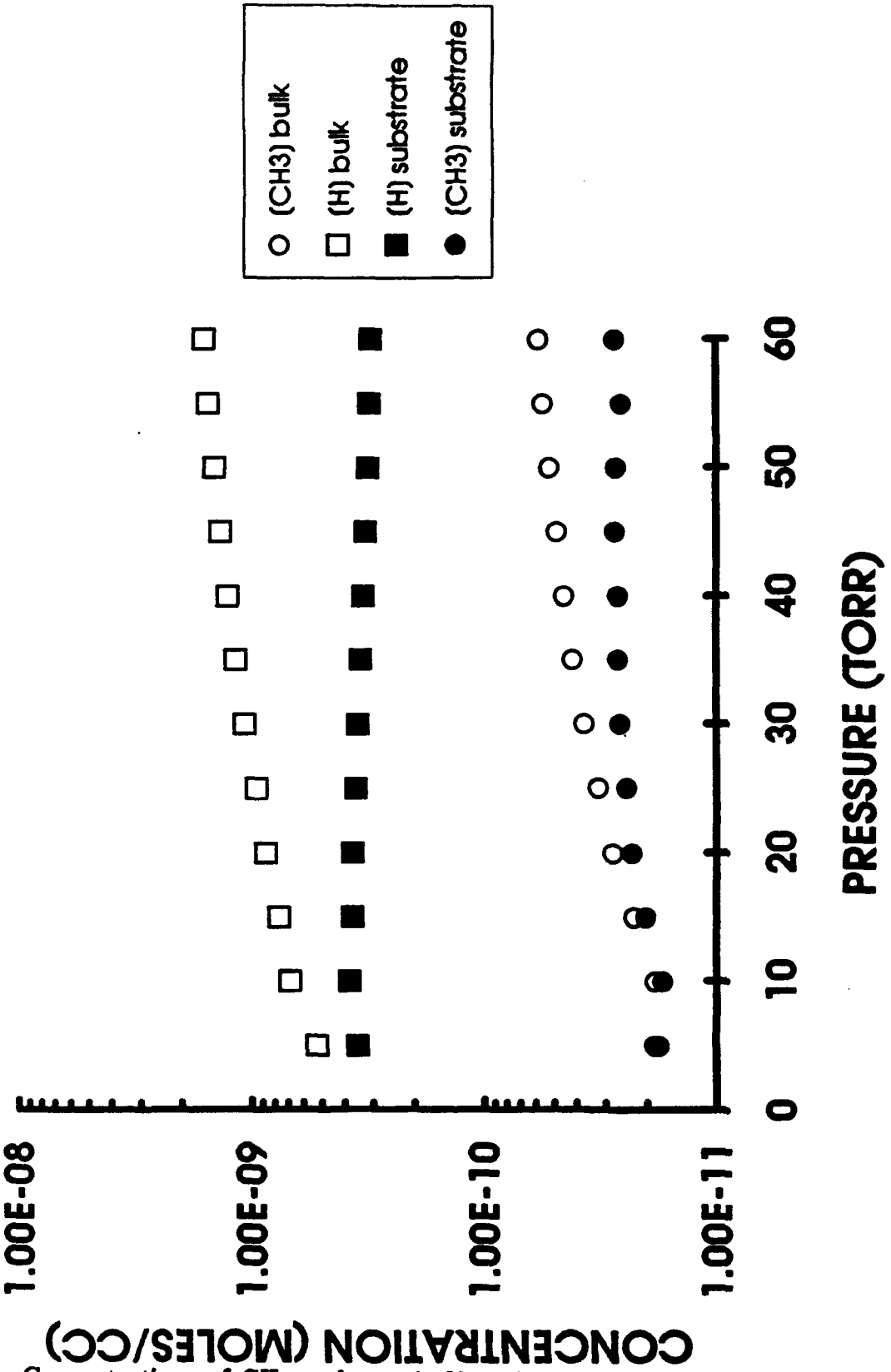

FIG. 7

7. Concentrations of CH_3 and atomic H as functions of gas pressure. Open symbols are bulk concentrations, far from any perturbation by a surface. Solid symbols are concentrations at the growth substrate.

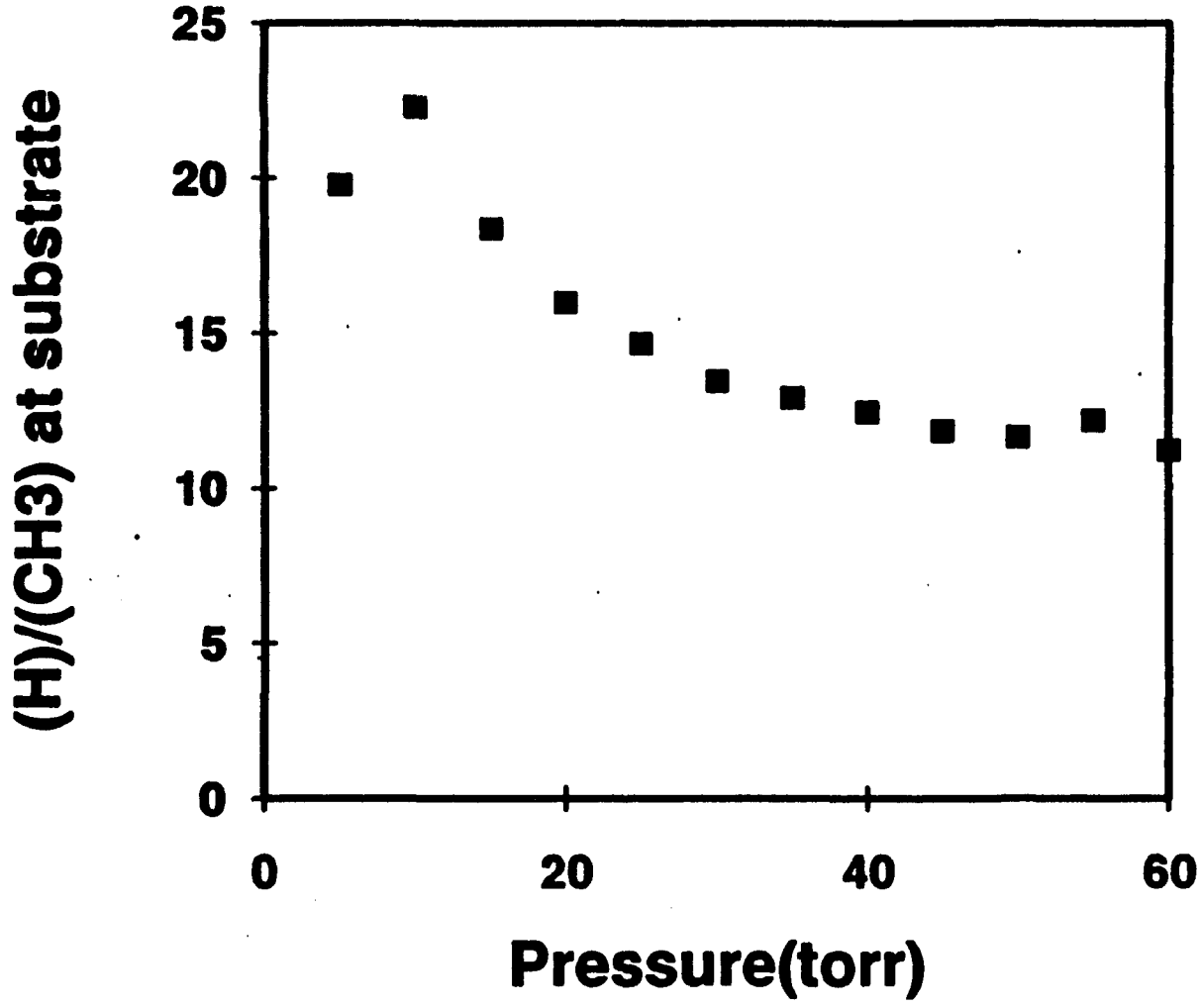
(H)/(CH3) at substrate
25
20
15
10
5
0
0
20
40
60
Pressure(torr)